Third Joint Eurohaptics Conference and Symposium on Haptic Interfaces
for Virtual Environment and Teleoperator Systems
Salt Lake City, UT, USA, March 18-20, 2009

Non-contact Tactile Sensation Synthesized by Ultrasound Transducers

Takayuki Hoshi[1], Takayuki Iwamoto[2], and Hiroyuki Shinoda[1]

[1] The University of Tokyo and [2] Canon Inc.

ABSTRACT

This paper describes a new tactile device which produces stress fields in 3D space. Combined with mid-air and/or 3D stereoscopic displays, this device provides high-fidelity tactile feedback for interaction with visual objects. The principle is based on a nonlinear phenomenon of ultrasound; acoustic radiation pressure. The fabricated prototype device consists of 324 airborne ultrasound transducers, and the phase and intensity of each transducer are controlled individually. The total output force within the focal region is 1.6 gf. The spatial resolution is 20 mm. The prototype can produce sufficient vibrations up to 1 kHz. An interaction system including the prototype is also introduced which tracks user's hand and provides suitable touch feeling.

KEYWORDS: Tactile display, Airborne ultrasound, Acoustic radiation pressure

INDEX TERMS: I.3.7 [Computer Graphics]: Three-Dimensional Graphics and Realism.Virtual Reality

1 INTRODUCTION

There has been a wide interest in mid-air and/or 3D displays and such displays have been seen in many SF movies [1]. People in the movies see and manually interact with touch screens or virtual objects floating in front of them. Recently, novel technologies are developed to render images hovering in air without special glasses. FogScreen [2] and Heliodisplay [3] use a thin layer of fog as a projection screen. Holo [4] provides floating images from an LCD by utilizing a concave mirror. SeeReal Technologies is working on a real-time, computer-generated, and 3D holography [5] through the use of an eye-tracking technology for reduction of calculation amount. Furthermore, by applying the camera-based and marker-less hand tracking techniques demonstrated in Holovizio [6] or GrImage [7], we will be able to handle the projected images with our hands. Then, tactile feedback will be the next demand. If tactile feedback is provided additionally, the usability of the interaction systems will be highly improved.

There are three types of conventional strategies for tactile feedback in free space. The first is attaching tactile devices on user's fingers and/or palms. Employed devices are, for example, vibrotactile stimulators (CyberTouch [8]), motor-driven belts (GhostGlove [9]), and pin-array units (SaLT [10]). In this strategy, the skin and the device are always in contact and that leads to undesired touch feelings. The second is controlling the position of tactile devices so that they contact with the skin only when tactile feedback is required. In the master-slave system shown in [11], the encounter-type force feedback is realized by the exoskeleton master hand. The detailed tactile feedback for each finger is provided by the electrotactile display attached on the finger part of the master hand. The drawback of this strategy is that it requires bulky robot arms. The last is providing tactile feedback from a distance without any direct contact. For example, air-jets are utilized in [12] to realize non-contact force feedback. Although air-jet is effective for rough "force" feedback, its spatial and temporal properties are quite limited and it cannot provide detailed "tactile" feedback.

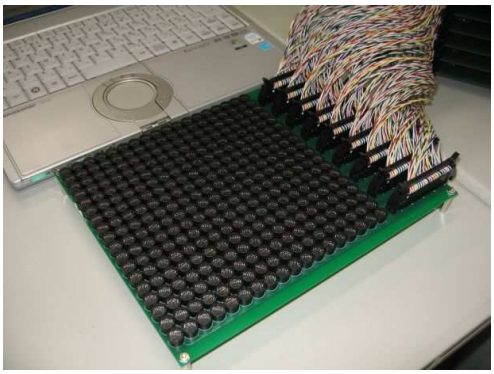

Figure 1. 18×18 array of ultrasound transducers

We have proposed a method for producing tactile sensation with airborne ultrasound [13]. The method renders desired pressure pattern in free space by using wave field synthesis with high spatial and temporal resolution. Users can feel the pressure with their bare hands. In [13], the prototype consisting of 91 ultrasound transducers was introduced and the feasibility of the proposed method was discussed. It can move a focal point only along Z axis. In this paper, we show an upgraded version of the prototype consisting of 324 ultrasound transducers (Figure 1), which can move a focal point three-dimensionally. The structure and performance of the device are described. An interaction system is also shown which tracks user's hand and provides tactile feedback according to the hand's position.

2 AIRBORNE ULTRASOUND TACTILE DISPLAY

2.1 Principle

Our method is based on a nonlinear phenomenon of ultrasound; acoustic radiation pressure. The acoustic radiation pressure P [Pa] is described as

$$P = \alpha E = \alpha \frac{I}{c} = \alpha \frac{p^2}{\rho c^2} \quad (1)$$

where E [J/m^3] is the energy density of the ultrasound, I [W/m^2] is the sound intensity, c [m/s] is the sound speed, p [Pa] is the RMS sound pressure of the ultrasound, and ρ [kg/m^3] is the density of the medium. α [-] is a constant ranging from 1 to 2 depending on the reflection coefficient R [-] at object surface; $\alpha \equiv 1 + R^2$. In case the object surface perfectly reflects the incident ultrasound, $\alpha = 2$,

Add.: Eng. Bldg. 6, 7-3-1, Hongo, Bunky-ku, Tokyo, Japan
E-mail: {star, iwa, shino}@alab.t.u-toyo.ac.jp

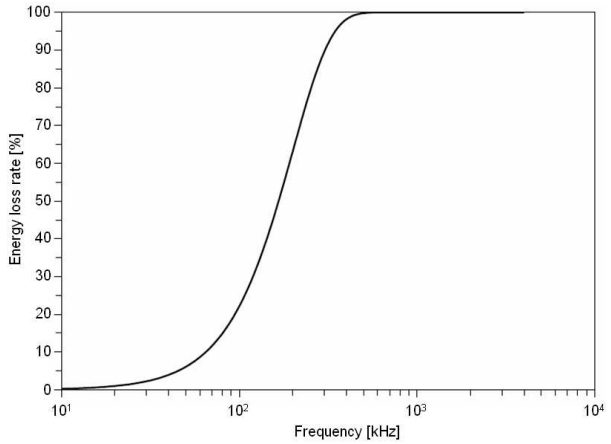

Figure 2. Relationship between ultrasound frequency and energy loss rate at 200 mm distance

while if it absorbs the entire incident ultrasound, $\alpha = 1$. The acoustic radiation pressure acts in the same direction of the ultrasound propagation. That is, roughly saying, the ultrasound "pushes" the object. Eq. (1) suggests that the spatial distribution of the pressure can be controlled by using wave field synthesis.

Air is a medium of ultrasound in this paper, unlike our previous study [14] in which water is used as a medium. In fact, air is a better selection compared with water from the viewpoint of engineering. The first difference is originated from the speed of sound. The pressure P is inversely proportional to the speed of sound c if the sound intensity I is same. c in air (= 340 m/s) is 4.4 times smaller than that in water (= 1500 m/s), and that leads to 4.4 times stronger acoustic radiation pressure. The second difference is originated from the reflection coefficient. The characteristic acoustic impedance of skin Z_s and that of air Z_a are 1.52×10^6 and 0.0004×10^6 N·s/m^3, respectively. (Note that it is assumed that the characteristic acoustic impedance of the skin is equal to that of water for simplicity.) In this case, the reflection coefficient R is calculated as,

$$R = \left|\frac{Z_s - Z_a}{Z_s + Z_a}\right| \approx 0.9989 . \tag{2}$$

Therefore, 99.8 % (= $R^2 \times 100$) of the incident acoustic energy is reflected at the skin surface. So, airborne ultrasound can be directly applied onto the skin without penetration. α in Eq. (1) is then almost maximized. On the other hand, almost all the incident acoustic energy of ultrasound propagating in water is absorbed to the skin because $R \approx 0$ at the interface between the skin and water, and hence an ultrasound reflective film is needed for safety [14].

The effective range and the spatial resolution of the proposed method are in the relation of trade-off. The higher the frequency of the ultrasound is, the smaller the diameter of the focal point of the ultrasound becomes. From the viewpoint of the spatial resolution, the smaller diameter is preferable. However, air is a lossy medium and its attenuation coefficient β [Np/m] for a plane sound wave is approximately proportional to the square of the frequency f^2. In this case, the energy density E at the distance z [m] is described as

$$E = E_0 e^{-2\beta z} \tag{3}$$

where E_0 [J/m^3] is the energy density at the transducer surface (i.e. $z = 0$ mm). Figure 2 shows the relationship between the frequency

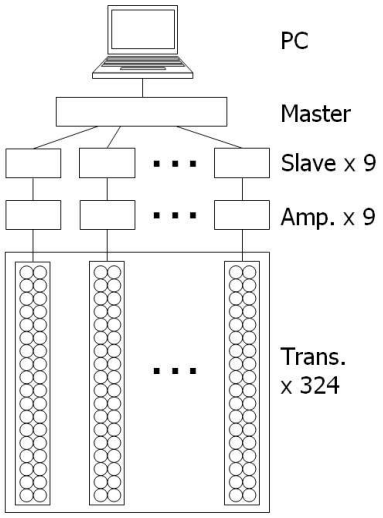

Figure 3. Block diagram of prototype device

of the ultrasound and the energy loss ratio when the sound reaches to $z = 200$ mm. For simplicity, it is assumed that the value of the attenuation coefficient β at 40 kHz is 100 dB/100m = 1.15×10^3 Np/m [15], and β is proportional to f^2 at the other frequencies. When the frequency of the ultrasound is 40 kHz, the energy loss is only 4 %. However, if the frequency becomes four times larger, the 50 % of the emitted acoustic energy is lost. Our prototype device utilizes 40 kHz ultrasound because the effect of the attenuation is relatively small and 40 kHz ultrasound transducers are commercially available.

Here we roughly estimate the total force produced with an ultrasound transducer array. The airborne ultrasound transducers are employed which are usually used for measuring distance or detecting objects. The sound pressure p' [Pa] of each transducer is 20 Pa at the distance of 300 mm. When all the phases of the ultrasound waves from N transducers match and one focal region is generated, the total sound pressure $p = Np$'. In air at room temperature, $\rho = 1.2$ kg/m^3 and $c = 340$ m/s. Assume the diameter of the focal region is equal to the wave length λ [m] (e.g. $\lambda = 8$ mm for 40 kHz ultrasound). According to Eq. (1), the total output force within the focal region is 3.0 gf when $N = 324$ and $\alpha = 2$. This estimated force is sufficient for producing vibratory sensation

2.2 Prototype Device

Figure 1 shows the array of airborne ultrasound transducers (T4010A1, Nippon Ceramic Co., Ltd.). The transducers are in a square arrangement. The diameter of each transducer is 10 mm. The resonant frequency is 40 kHz. The sound pressure emitted from the transducer is 20 Pa at 300 mm from the radiation surface.

Figure 3 shows the block diagram of the system. The system consists of a laptop PC with a digital I/O card (CBI-2701, Interface Corp.), a master circuit, 9 slave circuits, 9 amplifier circuits and the transducer array. The master circuit has an FPGA and a 25.6 MHz oscillator which acts as the system clock, and each slave circuit also has two FPGAs with two 4 Mbit SRAMs. The master circuit receives a command or data from the PC through the digital I/O, and broadcasts it to the slaves. Each slave drives 36 transducers individually through the 36-ch amplifier circuit. The driving signal into the transducer is a 24 Vp-p (the DC component is cut by a HPF), 40 kHz, and rectangular wave.

The system operates as follows. When the system is turned on, the pre-calculated look-up table of phase delays and amplitudes

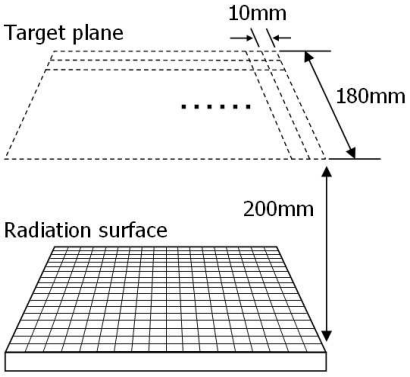

Figure 4. Description of target plane

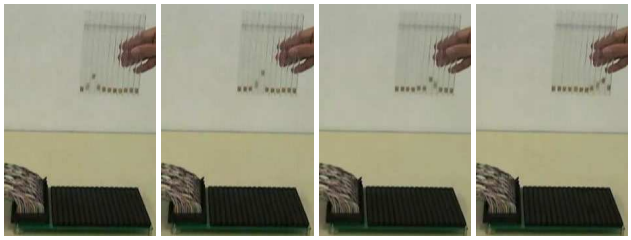

Figure 5. Left-to-right scanning movement of focal point

are downloaded to the slaves. After that, according to the command sent from the PC, the slaves drive the ultrasound transducers at the corresponding phases and amplitudes based on the table. The adequate look-up table is calculated from an objective spatial pattern by solving an inverse problem.

Hereinafter, we describe the specifications of the prototype. To control the phase and amplitude, one cycle of 40 kHz rectangular wave is divided in 16 segments (i.e. 1.5625 us). The phase is controlled by the position of a HIGH (= 24 V) period within the 16 segments, and the amplitude by the duration of the HIGH period (i.e. PWM). That is, the phase and amplitude are quantized in 4 and 3 bit, respectively.

The objective spatial pattern is limited to the single-peaked pattern, because the total force is weak (only 3.0 gf at the maximum) and not enough for some distributed pressure pattern. To reduce total data amount, target area is limited to a 180×180 mm^2 horizontal plane at 200 mm above the radiation surface. The target area is divided into 10×10 mm^2 sub-areas. The center positions of the sub-areas are selectable as the focal position (Figure 4). That is, the focal point can move among 18×18 discrete positions. For each focal position, the corresponding phases are determined by the distance between the positions of the focal point and the transducers. The amplitude is tentatively set as the maximum value (i.e. 50 % duty ratio). Figure 5 shows a demonstration of the scanning movement of the focal point. Small wooden pieces in acrylic tubes (10 mm diameter) are flipped up as the focal point comes.

The pressure is controlled not only spatially but also temporally. It can be modulated by rectangular wave whose frequency and duty ratio is ranging from 1 to 1000 Hz and 50 %, respectively. The frequency is quantized in 5 bit so that the selectable values are equally spaced on the logarithmic frequency scale.

The time-averaged power consumption of the whole system is about 70 W (measured); 35 W for the master and slaves and 35 W for the amplifiers and transducers. The total acoustic power of ultrasound is 13.3 W (theoretically calculated from the spec).

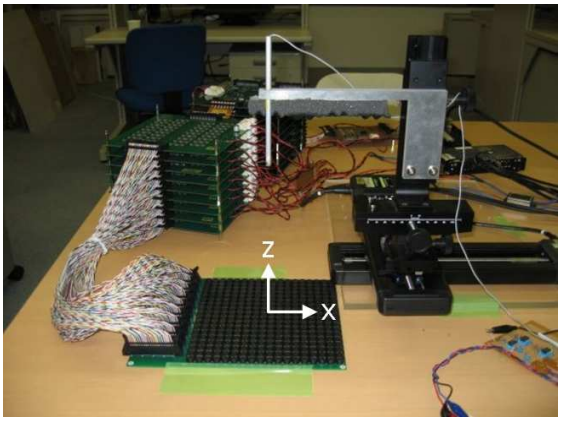

Figure 6. Experimental setup

3 EVALUATION

3.1 Total Force

The total force was measured using an electronic balance. The transducer array was fixed just above the electronic balance placed on a table. The radiation surface of the array was faced toward the electronic balance. (i.e. the radiation surface was upside down.) The ultrasound was continuously radiated without modulation during the measurement. The focal point was fixed at 200 mm above the radiation surface and the distance between the radiation surface and the electronic balance was also fixed at 200 mm. When the amplitude of the input signal was 24 Vp-p, the measured force was 1.6 gf, which is about half of the theoretical value estimated in Section 2.1. One possible reason is that not only the main lobe (focal point) but also side lobes and grating lobes are generated. Then the energy of ultrasound is shared among them. The directivity of the transducer and the incident angle of ultrasound may be also considerable.

3.2 Spatial Resolution

In order to measure the spatial distribution of the acoustic radiation pressure, we used a setup shown in Figure 6. An electret condenser microphone probe was attached to an XYZ stage. The microphone had little sensitivity to 40 kHz, and hence it was considered to measure the modulated acoustic radiation pressure. The resolution of the position of the XYZ stage was 0.1 mm. The aperture of the microphone was 2 mm. The focal point was fixed at the center of the array and 200 mm above the radiation surface. Data were acquired at every 2 mm around the focal region. The modulation frequency was 100 Hz, and the amplitude of the 100 Hz component was extracted from the stored data through the FFT. A digital oscilloscope (PCS-3200, Kenwood Corp.) was employed to sample data and to conduct the FFT calculation simultaneously. The amplitude was turned out to be time varying, and hence we recorded maximum and minimum values after 1 minute observing at each point.

Figure 7 shows the spatial distribution of the acoustic radiation pressure (100 Hz component) at z = 200 mm; (a) and (b) are the results of XY scanning and X scanning at y = 0 mm, respectively. The amplitude is normalized. Figure 7 (a) shows the maximum value within 1 minute observing time at each point and (b) shows the average values connected to each other and the maximum and minimum values as both ends of vertical bars. Three features are seen in Figure 7. First, the diameter of the focal region is about 20 mm. It is about twice larger than the wavelength of 40 kHz ultrasound (8 mm). Second, the side lobes are also seen around

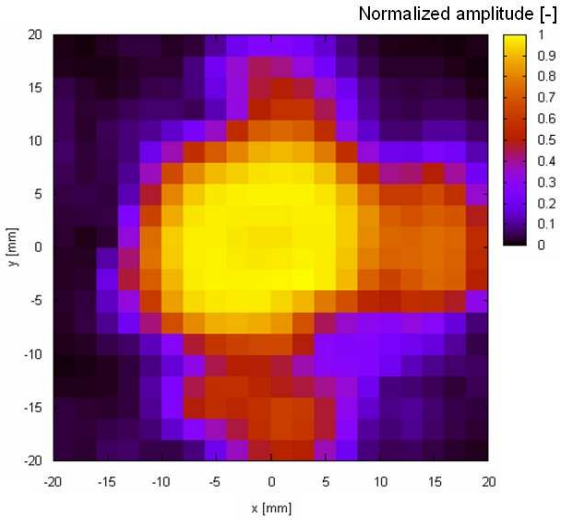

(a) Scanning along XY axes

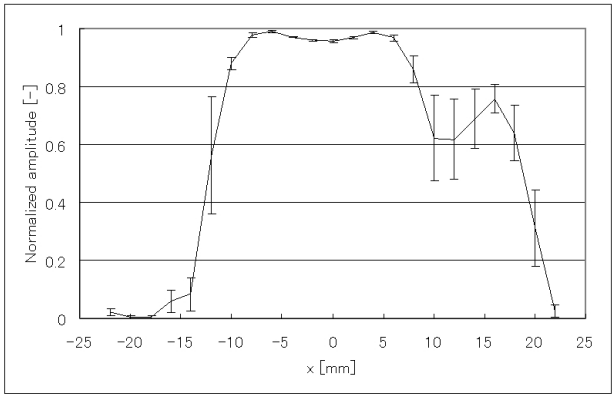

(b) Scanning along X axis (y = 0 mm)

Figure 7. Spatial distribution of measured radiation pressure

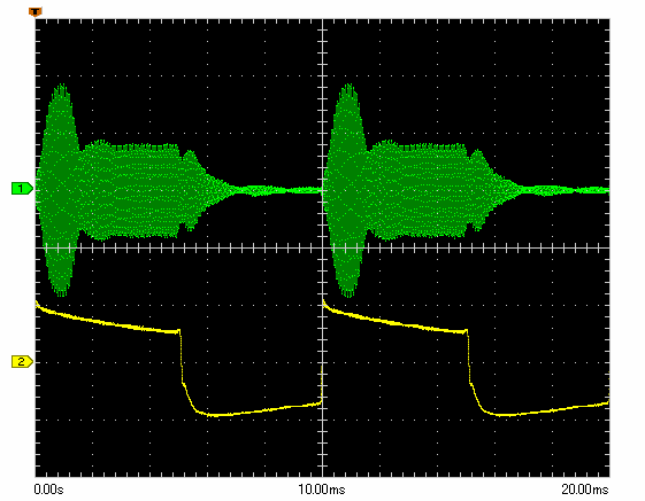

(a) 100 Hz modulated waveforms measured at focal point; ultrasound (CH1) and radiation pressure (CH2)

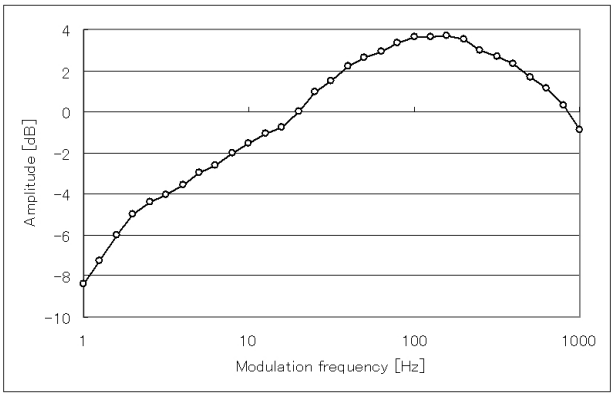

(b) Frequency characteristics

Figure 8. Temporal properties of measured radiation pressure

the main lobe. Third, while the radiation pressure inside of the focal region is stable, the outside is unstable due to an air flow.

3.3 Temporal Properties

Using the setup described in Section 3.2, the temporal properties of the radiation pressure were examined. The microphone was placed at the focal region. The ultrasound receiver (13 mm aperture, R4016A1, Nippon Ceramic Co., Ltd.) was also placed nearby the microphone in observing the ultrasound waveform shown in Figure 8 (a). The focal region was fixed at z = 200 mm. The driving signal was 40 kHz rectangular wave modulated by a rectangular wave whose frequency was changed.

Figure 8 (a) shows the waveforms of the ultrasound and the radiation pressure. The modulation frequency is 100 Hz. The vertical axis represents the measured voltage and its absolute value is not regarded here. The horizontal axis represents time. It is shown that the onset and end of the observed ultrasound waveform is unstable. The radiation pressure waveform is similar to a rectangular wave while it is not perfectly symmetric and decreases during each half cycle.

Figure 8 (b) shows the frequency characteristics of the radiation pressure. The horizontal axis represents the modulation frequency. The vertical axis represents the amplitude of the radiation pressure on a decibel scale. Here, the amplitude at 20 Hz is the 0 dB reference. While the carrier (ultrasound) frequency was fixed at 40 kHz, the sound power of ultrasound was modulated by each frequency. The measured amplitudes at 158 Hz and 1 kHz are 3.7 dB and -0.9 dB, respectively. The difference between them is only 4.6 dB (i.e. the amplitude at 158 Hz is 1.7 times larger than that at 1 kHz). From that, at least, it can be said that the frequency characteristics are flat between 20 Hz and 1 kHz. Note that the plots less than 20 Hz are not so reliable because the frequencies are out of the audible range of human where the performance of the microphone is uncertified.

3.4 Direction discrimination test

In order to confirm users can feel effective tactile sensation, a short experiment was conducted, in which the focal point was moved linearly (Figure 9). 6 volunteers (age range between 23 and 29 years, all male and right-handed) took part in the experiment. They held their right hands at 200 mm above the radiation surface of the transducer array (i.e. at the target plane). Two types of movement (distal-to-proximal and proximal-to-distal) were presented in a random order on their palm, and they were asked to answer the direction. Each direction was presented 20 times for one participant. The focal point moved 5 cm at a speed of 5 cm/s. The modulation frequency was 100 Hz. During the entire trials, the participants wore headphones and heard a white noise, which prevented them from hearing that 100 Hz audible sound.

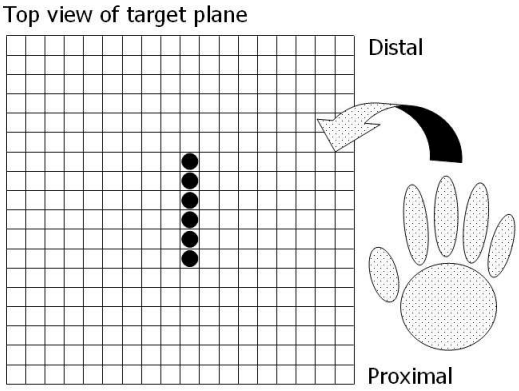

Figure 9. Trajectory of focal point in direction discrimination test (represented by black dots)

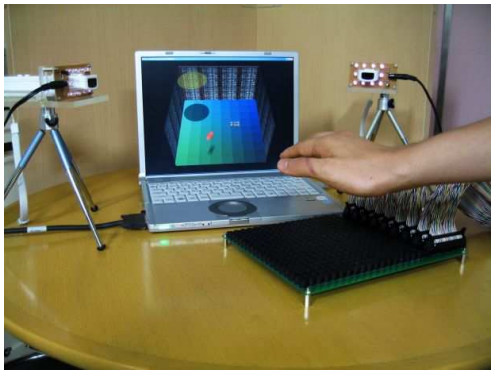

Figure 10. Interaction system consisting of airborne ultrasound tactile display and Wiimote-based hand tracking setup

As a result, all of the participants could discriminate the direction with 100 % accuracy. That indicates they could feel tactile sensation reliably enough to perform that task.

They also asked to give us feedback on tactile sensation they felt. Some of them reported slight sensation of an air flow just around the focal region. However the air flow was so weak and localized that they could easily detect the position of the focal region. The cause of the air flow can be the acoustic streaming or the difference of pressure generated by the acoustic radiation pressure. According to other reports on lower modulation frequencies, the onset of the radiation pressure seems to contribute to tactile sensation mainly. It may be possible to reduce the air flow and maintain the perceived intensity by decreasing the duty ratio of the modulation rectangular wave.

4 Interaction System

A preliminary interaction system was constructed by combining the proposed tactile display and a hand tracking setup. Because of cost, availability, and performance, we employed Wiimote (Nintendo) which has an infrared (IR) camera. A retroreflective marker is attached on the tip of user's middle finger. As shown in Figure 10, IR LEDs illuminate the marker and two Wiimotes sense the 3D position of the finger. This is only single-point tracking, but it is enough for our purpose at present.

The developed software is a "3D breakout game" (Figure 10). A virtual paddle controlled by the user's hand position is set at z = 200 mm. The user bounce a ball with the paddle to break bricks arranged at the bottom of a virtual room. When the paddle bounces the ball, a crash feeling is provided to the user's palm. The modulation frequency and duration are 100 Hz and 150 ms, respectively.

5 Conclusion

In this paper, a tactile display using airborne ultrasound was presented. The prototype could produce 1.6 gf within the focal region. The spatial resolution was 20 mm. The prototype could produce vibrations up to 1 kHz. Although the produced force was weak for users to feel constant pressure, it was sufficient for vibratory sensation. Hence, the prototype is expected to be useful for providing tactile cues in accordance with contacting virtual objects, or for producing texture sensation.

Now we are planning to combine the tactile display with some kind of mid-air visual display. We will also try to synthesize various texture feelings by controlling the spatial-temporal pattern of ultrasound.

References

[1] I. Rakkolainen: How feasible are Star Wars mid-air displays?, Proc. 11th International Conference Information Visualization (IV'07), pp. 935-942, 2007.

[2] FogScreen, http://www.fogscreen.com/.

[3] Heliodisplay, http://www.io2technology.com/.

[4] Holo, http://www.provision3dmedia.com/.

[5] Real-time holography, http://www.seereal.com/.

[6] T. Rodriguez, A. C. de Leon, B. Uzzan, N. Livet, E. Boyer, F. Geffray, T. Balogh, Z. Megyesi, and A. Barsi: Holographic and action capture techniques, Proc. 34th International Conference on Computer Graphics and Interactive Techniques (ACM SIGGRAPH 2007 Emerging Technologies), article no. 11, 2007.

[7] J. Allard, C. Menier, B. Raffin, E. Boyer, F. Faure: Grimage: Markerless 3D interactions, Proc. 34th International Conference on Computer Graphics and Interactive Techniques (ACM SIGGRAPH 2007 Emerging Technologies), article no. 9, 2007.

[8] CyberTouch, http://www.immersion.com/.

[9] K. Minamizawa, S. Kamuro, S. Fukamachi, N. Kawakami, and S. Tachi: GhostGlove: Haptic existence of the virtual world, Proc. 35th International Conference on Computer Graphics and Interactive Techniques (ACM SIGGRAPH 2008 New Tech Demos), article no. 18, 2008.

[10] S.-C. Kim, C.-H. Kim, T.-H. Yang, G.-H. Yang, S.-C. Kang, D.-S. Kwon: SaLT: Small and lightweight tactile display using ultrasonic actuators, Proc. 17th IEEE International Symposium on Robot and Human Interactive Communication (RO-MAN 2008), pp. 430-435, 2008.

[11] K. Sato, K. Minamizawa, N. Kawakami, S. Tachi: Haptic Telexistence, Proc. 34th International Conference on Computer Graphics and Interactive Techniques (ACM SIGGRAPH 2007 Emerging Technologies), article no. 10, 2007.

[12] Y. Suzuki and M. Kobayashi: Air jet driven force feedback in virtual reality, IEEE Computer Graphics and Applications, vol. 25, pp. 44-47, 2005.

[13] T. Iwamoto, M. Tatezono, and H. Shinoda: Non-contact method for producing tactile sensation using airborne ultrasound, Proc. EuroHaptics 2008, pp. 504-513, 2008.

[14] T. Iwamoto and H. Shinoda: Two-dimensional scanning tactile display using ultrasound radiation pressure, Proc. Symposium on Haptic Interfaces for Virtual Environment and Teleoperator Systems (IEEE Haptics Symposium 2006), pp. 57-61, 2006.

[15] H. E. Bass, L. C. Sutherland, A. J. Zuckerwar, D. T. Blackstock, and D. M. Hester: Atmospheric absorption of sound: Further developments, Journal of the Acoustical Society of America, vol. 97, pp. 680-683, 1995.